Rotor fault detection of electrical machines by low frequency magnetic stray field analysis

Olivier Chadebec, Viet Phuong Bui, Pierre Granjon, Laure-Line Rouve, Nicolas Le Bihan, Jean-Louis Coulomb

SDEMPED 2005 - International Symposium on
Diagnostics for Electric Machines, Power Electronics and Drives
Vienna, Austria, 7-9 September 2005

Rotor fault detection of electrical machines by low frequency magnetic stray field analysis

Olivier CHADEBEC[(1)], Viet Phuong BUI[(1)], Pierre GRANJON[(2)],
Laure-Line ROUVE[(3)], Nicolas LE BIHAN[(2)], Jean-Louis COULOMB[(1)(3)]
[(1)] LEG - UMR 5529 - INPG/UJF-CNRS - ENSIEG - BP 46 - 38402 Grenoble - France
[(2)] LIS - UMR 5083 - INPG/UJF-CNRS - ENSIEG - BP 46 - 38402 Grenoble – France
[(3)] LMN – INPG - ENSIEG - BP 46 - 38402 Grenoble – France

***Abstract* – This paper shows the reliability of fault detection on electrical machines by analysis of the low frequency magnetic stray field. It is based on our own experience about magnetic discretion of naval electrical propulsion machine. We try to apply the techniques developed in previous works on the subject to faults detection. In this paper we focus on rotor defaults in a synchronous generator (eccentricity and short-circuit in rotor). Two kinds of study are performed. The first one is numerical. Firstly, an adapted Finite Elements Method is used to compute the stray field around the device. However, this approach is difficult to apply to fault detection and not well-adapted. A new model, simpler and faster, is developed. Results are compared for both modelling. The second one is experimental and is driven thanks to a laboratory machine representative of a real high power generator and to fluxgate magnetometers located around the device. Both studies show good agreement and demonstate the reliability of the approach.**

I. INTRODUCTION

Full naval electrical propulsion architecture has several advantages compared to conventional drives (flexibility and better performances at low rotational speeds). This kind of technology is now widely used for both civilian and military ships, electrical machines being fitted inside a pod (i.e. outside the hull). However, for military applications, this solution is not without any consequences. Indeed, such electrical machines create stray magnetic field around the ship which can lead to its destruction by magnetic mines. For more than ten years, the Laboratoire de Magnétisme du Navire (LMN) and the Laboratoire d'Electrotechnique de Grenoble (LEG) have developed numerical tools and measurement processes to evaluate this radiated field. According to our own experience, the magnetic stray field generated by an electrical machine can give important information about its internal behaviour. In particular, defaults can have an important influence on this external stray field. This paper shows how the techniques developed by our researches in magnetic discretion can be applied to fault detection.

Magnetic stray field due to an electrical device can be modelled with an equivalent multipolar source by using the spherical harmonics theory [1]. In other words, the stray field can be represented by a sum of several terms presenting different laws of field's decrease. If we consider that r is the distance between the centre point of the device and the measurement point, the induction around the device is the sum of:

- a dipolar term (order 2) with a decrease of $1/r^3$
- a quadrupolar term (order 3) with a decrease of $1/r^4$
- an octopolar term (order 4) with a decrease of $1/r^5$
- etc...

Some of these terms can vanish. For instance, the dipolar term for a "perfect"4-poles electrical motor is equal to zero. Its stray field can be represented by a main quadrupolar term and higher order terms. However, if a default occurs in this device, electrical sources inside the motor loose their symmetry and a dipolar term appears. This point is determinant concerning the relevance of the fault detection by stray field measurement. Indeed, if sensors are placed far enough from the device, only the dipolar term is measured (see the decreasing laws). In fact, only the magnetic signature of the default will appear.

This preliminary consideration enforces us to believe that this approach is relevant. However, fault detection by magnetic measurements is not so simple. The main difficulty comes from the difference between the magnetic induction inside and outside the machine: a ratio of 1 to 10^{-6} is commonly encountered (1-2T in the machine against some μT outside). This very low level of induction leads to the development of specific measurement techniques and the use of adapted signal processing analysis.

The first part of the paper deals with a new model which allows to predict the stray magnetic field created by an electrical machine. This simple model is based upon the physical laws governing the behaviours of the device. Results obtained are then compared to those obtained by classical Finite Element analysis. Several examples are shown for different operating conditions (with or without defaults). Then, the reliability is validated by measurements on a laboratory synchronous generator.

II. A SIMPLE MODEL TO PREDICT THE STRAY MAGNETIC FIELD

A. FEM analysis

Lots of numerical models have already been developed to predict the stray magnetic field generated by electrical machines. Most of them are based on Finite Element Method (FEM). These approaches are now well-known to model healthy electrical machines in 2D or 3D. The machine and the surrounding air region are meshed by taking into account geometrical and physical symmetries of the devices. 2D models are the easiest to implement, where only a part of the section of the machine is taken into account. The magnetic induction in the device is then computed with a very good accuracy. However, the computation of the outside magnetic field encounters severe difficulties. First of all, the mesh in the air region must be very fine to avoid numerical noise due to the mesh. This point increases the memory and the CPU time needed for computation. A good solution is to use a dedicated numerical tool called "infinite box" which allows to compute the stray field quite accurately by modelling boundary condition at the infinite by conformal transformation [2]. Another difficult point is the simulation of the rotor motion which needs a new mesh at each time step. Finally, for 2D modellings, the length of the motor is considered as infinite. Even if a qualitative representation of the field's behaviour is obtained, its modulus is provided with mistakes. The good solution is often to provide a 3D modelling. However these numerical models are still rare in the literacy [3] and problems mentioned before are increased. A good solution is then to use a post-processor based on the moment method which has already shown good results validated by measurements [4].

For the case of faulty conditions, the electrical machine looses its natural symmetry, and modelling of the whole geometry is thus necessary. Even if some 2D uneasy modellings can be provided, 3D modelling is still impossible to manage.

To overpass this difficulty, we present a simple 3D model easy to implement which allows to predict the magnetic stray field of a machine. This model has the advantage to be sufficiently simple to allow the introduction of faults easily.

B. Modelling of a healthy machine

Consider an electrical machine made of windings, an air gap, a stator and a rotor. The stray magnetic field outside the device is created by the sum of:

- the field created by magnetisation of ferromagnetic parts (stator and rotor)
- the field created by currents in windings

1. Field due to magnetisation

Denote V a ferromagnetic body that channels a flux of induction (high magnetic permeability). The field created by this device can be computed by the well-known expression:

$$B(x) = \mu_0 \iiint_V g(\mathbf{M}(x'))dV \qquad (1)$$

where x is the measurement point, x' is the integration point and g is the mathematical expression of the field created by a dipole.

In such a case, it is usual to consider that in this volume, **M** has a free divergence. The volume V creates exactly the same field as a surface S with a charge distribution q=**M**.**n**, where **n** is the normal going outside from the volume. More precise explanations of this representation can be found in [5].

Then, the field can be computed by:

$$B(x) = \mu_0 \iint_S f(\mathbf{M}(x').\mathbf{n}(x'))dS \qquad (2)$$

where f is the mathematical expression of the field created by a charge. This approach is called Coulombian representation of a ferromagnetic body.

In the example presented in Fig. 1, volume V channels perfectly the flux of induction. Charges located on all the faces where **M** is perpendicular to the normal vanish. Only two opposite charges remain at the top and bottom of the volume.

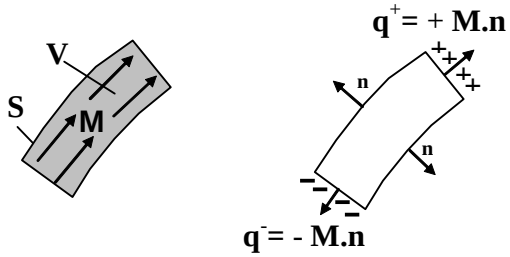

Figure 1: Representation of a magnetized volume and its equivalent surface charge distribution. Both magnetic fields computed are the same.

Consider now the field created by the stator and the rotor of an electrical machine. Fig.2 shows the Coulomb representation applied to this device. We consider that permeability of rotor and stator are high and that the field is well channelled by the ferromagnetic material. Charges only appear on surfaces where the field is going from the ferromagnetic region to the air one (i.e. on the two interfaces I1 and I2 delimiting the air gap). Two charge distributions with opposite signs are thus obtained on the two previous interfaces.

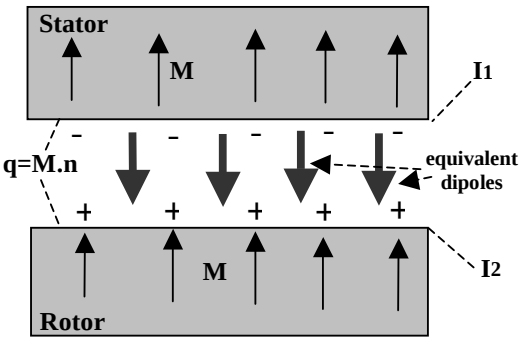

Figure 2: Representation of the magnetic circuit. It could be represented by two layers of charges with opposite signs close to each other (i.e. a simple layer with normal dipoles located on the average surface of the air gap).

The charges value q depend on the field in the air gap. By applying Ampere's law and by considering that the field in

the ferromagnetic part is equal to 0 (high permeability), the value obtained for q is:

$$q = B_{airgap} \times \frac{\mu_r - 1}{\mu_0 \mu_r} \quad (3)$$

The field created by the ferromagnetic material can be represented by a surface distribution **T** of normal dipoles located on the average surface of the air gap of the machine.

$$T_{mag} = e \times B_{airgap} \times \frac{\mu_r - 1}{\mu_0 \mu_r} \quad (4)$$

where e is the thickness of the air gap. T is called a double layer potential surface. For example, let us consider a p-poles electrical machine with a sinusoidal air gap induction. The field created by ferromagnetic parts is almost the same as the field created by the following cylindrical surface distribution of normal dipoles:

$$T_{mag}(\theta,t) = e \times \frac{\mu_r - 1}{\mu_0 \mu_r} \times B_{airgap\_max} \times \cos(p\theta - \omega_s t) \quad (5)$$

where θ is the mechanical position of the rotor and ω_s is the electrical pulsation.

2. Field due to the windings

Let us now consider a single loop C in which flows a current I. The magnetic field created by this current is the same as the one created by every surface S delimited by C with a dipole distribution equal to I.**n,** where **n** is the normal to the surface [5]. It is easy to see that such a surface dipole distribution is equivalent to the line current. To this end, we consider a network of small loop currents. The contributions of all currents cancel each other except on the line C. If the sizes of the small loops tend to 0, we get a distribution of current vortex equivalent to dipoles. This result is known as the Ampere equivalence (see Fig. 3).

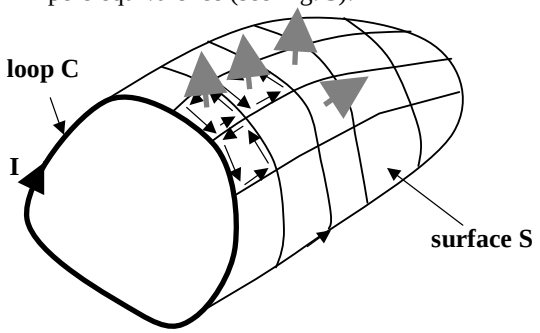

Figure 3: Equivalence between the current flowing in a winding and a distribution of normal dipoles

We can apply this result to the rotor winding, lines C being the coils and the surface S being the average surface of the airgap. In most part of an electrical machine, the sum of the different I.**n** dipoles created by all the windings can be considered, in a first approximation, as sinusoidal. By neglecting the end-windings effects, one can then model the field created by the winding as a distribution of normal dipoles located on the cylindrical average air gap surface. Its expression is:

$$T_{wind}(\theta,t) = -A_{t\_max} \times \cos(p\theta - \omega_s t) \quad (6)$$

where A_{t_max} is the maximum number of Ampere-turn for one pole.

3. Complete model

We get thus a model which takes into account both ferromagnetic and windings effects. The model is a cylindrical surface with a distribution of normal dipoles on it, which is the sum of T_{mag} and T_{win}:

$$T(\theta,t) = k \times \cos(p\theta - \omega_s t) \quad (7)$$

where k is a coefficient depending on expression (5) and (6). Some remarks must be pointed out about this model. First, T_{wind} and T_{mag} have opposite directions. In others words, T_{wind} creates de source field and T_{mag} represents the shielding effect of the ferromagnetic materials. Obviously, this representation is an approximation. In fact, many other charges appear everywhere in the stator and the rotor. However, charges on the surfaces delimiting the air gap are the most significant. Even if this model cannot allow to compute the stray field very accurately, it leads to a correct qualitative approximation.

4. Numerical implementation

We consider a cylindrical surface meshed into 520 rectangular elements with uniform normal dipoles distribution. The surface distribution T depends on the angular position and the time and is calculated by using equation (7). Note that in this model the mesh does not have any motion. The model is thus easy to implement. Once the value of each dipole at each time step is obtained, the field created on a sensor located somewhere in the air region can be calculated thanks to a relation similar to (1). The computation of this integral is provided by Gauss numerical integration method.

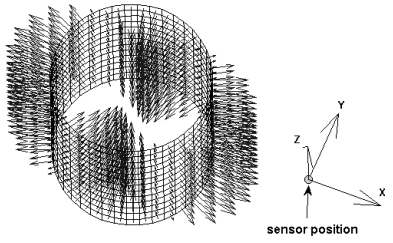

Figure 4: Mesh of the air gap (520 elements), dipoles distribution obtained with a healthy 4 poles machine and magnetic sensor position.

III. NUMERICAL RESULTS

In this section, the previous model is applied to a synchronous generator with stator windings in open circuit mode. The model is tested for a healthy machine and different rotor faults. The results are compared to those obtained by a standard FEM analysis.

A. Presentation of the laboratory machine

A 30 kVA synchronous generator [6] driven to a constant speed by a DC machine is used in order to check the previous model on a real machine. This generator has four parallel

windings per phase, 4 poles and 48 stator slots. The excitation winding is divided into three parts. The first part is made of one-ninth of the first pole, the second part is made of the remaining eight-ninths and the last part is made of the three others poles. The two ends of each winding are connected to switches in order to create different electrical rotor faults. In this study, we are looking for rotor faults such as short-circuit in rotor and dynamic mechanical eccentricity, while the stator windings are in an open circuit state. The rotation speed of the machine is 150 rounds per minute, which corresponds to a synchronous frequency of f_s = 5 Hz.

B. Finite element modelling

The geometry of this machine has been designed in Flux2d software (see Fig. 4). The machine loosing its symmetries in a faulty state, we need to represent its whole geometry. A virtual magnetic sensor is placed at 100mm from the machine in the air region. Notice that the important result is the magnetic field in the air region which is not taken into account in usual modellings. Therefore, we need to use a special numerical tool called "infinite box" which allows to compute the stray field quite accurately as it is explained in the first part.

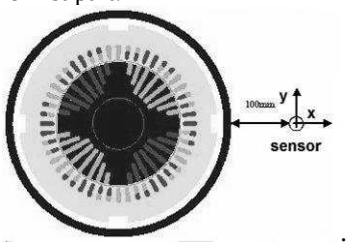

Figure 4: Geometry of the synchronous machine and sensor location

C. Some examples

As seen previously, the distribution of dipoles is directly proportional to the field in the air gap. If we have an image of this field, we can, thanks to our model, predict the behaviour of the field outside.

1. Healthy machine

The field in the air gap of a healthy synchronous machine mostly contains a main sinusoïdal component with frequency f_s, added with its odd harmonics which are due to windings effects. However, a more accurate representation must take into account the stator slots effect. Therefore, we use the dipole distribution expression given by [7]:

$$T(\theta,t) = \sum_{n=1,3,5} T_{0n} \times \cos(n(p\theta - \omega_s t)) \times (1 + \varepsilon \cos(n(k/p \times ((p\theta - \omega_s t))) \quad (8)$$

where p is the pole pair number, $\omega_s=2\pi f_s$ is the synchronous pulsation, k is the total number of stator slots and ε denotes the reluctance variation due to stator slots. By neglecting the slots and windings effects (ε=0, n=1), the previous distribution T(θ,t) can be represented by the rotation of four dipoles at the rotating pulsation $\omega_s/2$ (see Fig. 5):

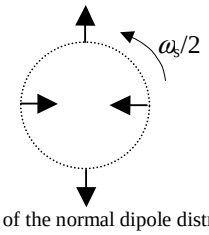

Figure 5: Representation of the normal dipole distribution obtained with a healthy machine (only maximal values are represented)

This model shows that the stray magnetic field of the machine can be approximated by the rotation of a quadrupole at the rotation speed. In this case, the spectrum of this field will be constituted by a spectral line with a frequency of 5 Hz.

Thanks to the finite element analysis, we obtain the frequency spectrum of the stray field on the sensor (see Fig. 6).

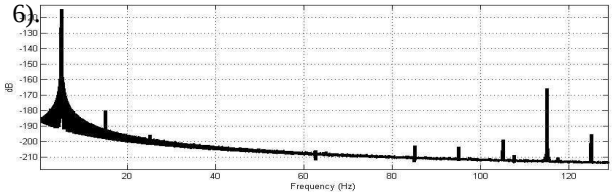

Figure 6: Frequency spectrum of the stray field for the healthy machine obtained with finite element analysis.

The first and major component with a frequency of 5Hz=f_s represents poles rotation as explained before. Small components of frequency 15Hz=$3f_s$ and 25Hz=$5f_s$ are due to windings effect. Components of frequency 115Hz (k/p-1=48/2-1=23rd harmonic of f_s) and 125Hz (k/p+1=48/2+1=25th harmonic of f_s) represent the modulation of the field in the air gap by the k=48 stator slots.

Thanks to our model (Eq. (8) coupled with Eq. (1)), we obtain the following spectrum which presents a good adequacy with the FEM analysis (only 1st and 3rd windings effect components are taken into account here).

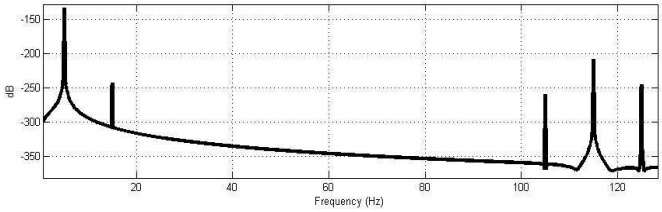

Figure 7: Frequency spectrum of the stray field for the healthy machine obtained with normal dipoles surface model (n=1 and n=3).

This result validates our approach and the previous simple model is used in the following in order to predict stray field of the faulty machine. Moreover, this work only deals with rotor fault diagnosis by analysing low frequency components of the stray magnetic field, so that the slot effect is neglected in the sequel.

2. Rotor short-circuit

We introduce now a one-ninth short circuit of one pole of the rotor windings. The dipole distribution is thus given by [7]:

$$T(\theta,z) = \sum_{n=1,3,5,...} T_{0n} \times (\cos(n(p\theta - \omega_s t)) + \sum_{m=1,2,3,4...} \lambda_{ccm} \cos(m(\theta - \omega_s t/p)) \quad (9)$$

where λccm is a constant linked to the fault amplitude. Let us notice that the turn to turn short-circuits adds a new term with a rich harmonic decomposition of frequency mf_s where m=1,2,3,4…

This model can thus be represented as follows:

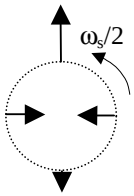

Figure 8: Representation of the normal dipole distribution obtained with a windings default in the rotor (only maximal values are represented)

which is the sum of two more simple representations:

- one quadrupole, representative of the healthy machine (magnetic signature in $1/r^4$ – n=1)
- a more complex term with a very rich harmonic decomposition (m=1,2,3,4,…). The presence of the fourth harmonic in the magnetic field is due to the strong dissymmetry of the windings (rotation of a single coil at the rotor speed).

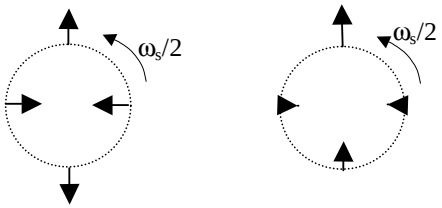

Figure 9: Representation of the normal dipole distribution obtained with a winding fault in the rotor (only maximal values are represented). This representation is the sum a quadrupole and a more complex term.

Thanks to this model, we obtain the following spectrum:

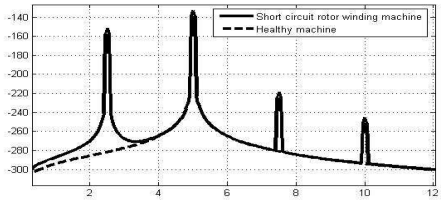

Figure 10: Frequency spectrum of the stray field obtained by the normal dipoles surface model – Comparison between healthy machine (dashed line) and short-circuit rotor windings machine (simple line).

This figure shows that in this case, the stray magnetic field is composed by the healthy machine component (f_s=5Hz), added with other spectral lines. These components, generated by the rotor winding short circuit, are located at frequencies $f_s/2$, $3f_s/2$, and $2f_s$, as predicted by Eq. (9).

3. Dynamic eccentricity of the rotor

A dynamic eccentricity is now introduced in the numerical model. The dipole distribution becomes:

$$T(\theta,z) = T_0 \times \cos(p\theta - \omega_s t) \times (1 + \lambda_{ed} \sin(\theta - \omega_s t/p)) \quad (10)$$

where λ_{ed} represents the eccentricity magnitude. This distribution can be simply represented by:

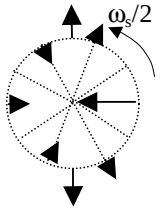

Figure 11: Representation of the normal dipole distribution obtained with a dynamic eccentricity of the rotor (only maximal values are represented).

which corresponds to the sum of three distributions:

- the rotation of a quadrupole, representative of the healthy machine (magnetic signature in $1/r^4$)
- the rotation of two dipoles (magnetic signature in $1/r^3$)
- the rotation of an octopole (magnetic signature in $1/r^5$)

which will be importantly attenuated because of its strong decreasing law.

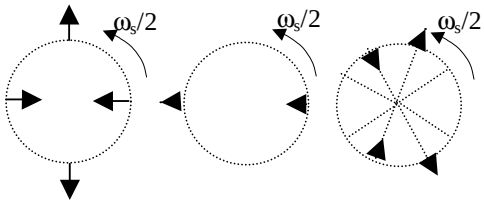

Figure 12: Representation of the normal dipole distribution obtained with a dynamic eccentricity of the rotor (only maximal values are represented). This representation is the sum a dipolar term, a quadrupole one and an octopole one.

Thanks to this model, the following spectrum is obtained:

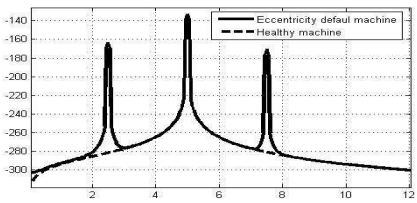

Figure 13: Frequency spectrum of the stray field obtained by the normal dipoles surface model – Comparison between healthy machine (dashed line) and a rotor dynamic eccentricity (plain line).

In this case, the stray magnetic field is composed of the healthy machine component (f_s=5Hz), added with two side band components. They are genenerated by the dynamic rotor excentricity which induces amplitude modulation with a frequency $f_s/2$ (see Eq. (10)). Therefore, the frequency of the additive components generated by this kind of rotor fault are the same as in the rotor winding short circuit case, unless the component at 10Hz=$2f_s$ which can be used to discriminate the two previous faults.

IV. EXPERIMENT

This experiment was carried out on the laboratory

machine previously described (a 4 pole, 30 kVA synchronous generator with 48 stator slots). This generator was driven to a constant rotation speed of 150 rounds per minute by a DC machine, and the corresponding synchronous frequency was $f_s = 150/60 \times 2 = 5$ Hz. A magnetic flux gate sensor was placed at 100 mm from this machine. The output of this magnetic sensor represents the stray magnetic field of the generator in the radial direction. During operation, the stator windings were in an open circuit state, such that the flux gate sensor only measured the magnetic field generated by rotor (excitation) windings. This measured quantity was low-pass filtered and sampled such that the obtained numerical signal verified the Shannon's sampling theorem.

Two different experiments were carried out:

- one with healthy rotor windings,
- one with a one-ninth short circuit of one pole of the rotor windings.

Then, the power spectra of the measured magnetic fields were estimated in the low frequency band (0-12 Hz) by employing the Welch's modified periodogram estimation method (block-averaging). The results are shown in Fig. 15, were the dashed line represents the magnetic field spectrum in the healthy case, and the plain line the magnetic field spectrum in the short circuit case.

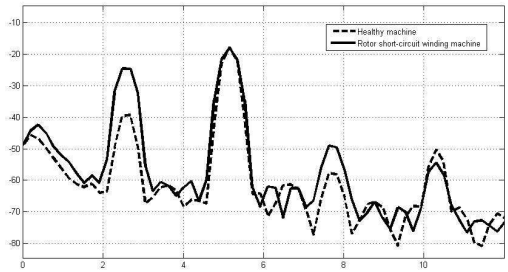

Figure 15: Frequency spectra of the measured stray magnetic field.

In the healthy case, the main component of this spectrum is located at $f_s = 5$ Hz as predicted by our model (see Fig. 7). However, small additional components appear at 2.5 Hz, 7.5 Hz and 10 Hz, which are representative of short circuit rotor windings (see Fig. 10). This surprising result is due to the lamination of the ferromagnetic steels of this machine which is not isotropic (steels are probably not assembled in an optimal manner). As a result, the stator reluctance is not the same in all directions and the generated flux is similar to the one created by rotor windings with a very small short circuit. As noticed in Fig. 15, these additional components are small compared to the main component (20 dB less).

In the faulty case, the spectral lines of frequency 2.5 Hz and 7.5 Hz increase importantly (of about 10 dB). These components are induced by the rotor windings short circuit as predicted by our model (see Fig. 10). Unfortunately, they have the same frequencies as the ones induced by a dynamic mechanical eccentricity (see in Fig. 13).

Therefore, a rotor fault can be easily detected thanks to classical spectral analysis of the stray magnetic field around the synchronous frequency, but the type of fault can't be easily determined.

IV. CONCLUSION

In this paper, a simple model of the stray magnetic field of a synchronous machine has been determined. It is based on the representation of the airgap magnetic field by a dipole distribution, and takes into account the attenuation effect of the magnetic field in the air region. A finite element method analysis has been used to show that this simple model correctly represents the magnetic field outside the machine in a qualitative manner, and is able to precisely predict its frequency contents.

This model has been employed in order to theoretically predict the stray magnetic field generated by a synchronous generator in the case of different rotor faults (short circuit rotor windings and dynamic mechanical eccentricity). Classical spectral analysis has been applied on predicted and measured stray magnetic field around the synchronous frequency of the machine (low frequency band) in order to analyse their frequency contents. The results has shown that this technique can be employed as an efficient rotor fault *detector*, but not yet in order to *discriminate* the different types of rotor faults.

To this end, several ways are still to be investigated. Firstly, the frequency contents of the stray magnetic field can be analysed in the high frequency band, and particularly around the slot lines in order to find additional information. More sophisticated signal processing techniques can also be used on this signal, such as time frequency representations. Secondly, the analysis method can be applied to the three dimensions of the measured magnetic field instead of using only one dimension (only the radial direction has been considered in this work). Indeed, some geometrical information about the measured magnetic field could then be determined and used to discriminate different types of faults. Finally, the stray magnetic field can be used in order to reconstruct the magnetic field in the airgap. Indeed, this quantity is particularly interesting because it does not undergo the attenuation effect due to the air region.

V. REFERENCES

[1] J.P. Wikswo, Jr. And K.R., Swinney, *Scalar multipole expansions and their dipole equivalents*, J. Apl. Phys. 55, 3039, 1984

[2] X. Brunotte, G. Meunier, J. F. Imhoff "*Finite elements solution of unbounded problems using transformations: a rigorous, powerful and easy solution", IEEE Trans. Magn.*,Vol. 28, pp 1663-1666, March 1992.

[3] O. Mun Kwon, C. Surussavadee, M. Chari, S. Salon, K. Sivasubramaniam, "*Analysis of far field of permanent-magnet motors and effects of geometric asymetries and unbalance in magnet design,*" IEEE Trans. Magn, Vol. 40, No 2,pp 435-442, March 2004.

[4] B. Froidurot, L-L. Rouve, A. Foggia, J-P. Bongiraud, G. Meunier, "*Magnetic discretion of naval propulsion machines*," IEEE Trans. Magn, Vol 38 , No 2 , pp 1185 - 1188, March 2002.

[5] E. Durand, Magnétostatique, Masson et Cie, Paris, 1968

[6] J-E. Torlay, A. Foggia, C. Corenwinder, A. Audoli, J. Herigault, *Analysis of shaft voltage and circulating currents in the parallel-connected winding in large synchronous generators*, Electric components and system, Vol 30, No 2, 2002, pp 135-149.

[7] P. L. Timar. *"Noise and Vibration of Electrical Machines,"* Elsevier Science, New York, 1989.